



# Snow shielding factors for cosmogenic nuclide dating inferred from Monte Carlo neutron transport simulations



Christopher Zweck<sup>a,\*</sup>, Marek Zreda<sup>a</sup>, Darin Desilets<sup>b</sup>

<sup>a</sup> Department of Hydrology and Water Resources, University of Arizona, Tucson, AZ 85721, United States

<sup>b</sup> Sandia National Laboratories, Albuquerque, NM 87185, United States

## ARTICLE INFO

### Article history:

Received 12 June 2012

Received in revised form 7 July 2013

Accepted 16 July 2013

Available online 28 August 2013

Editor: G. Henderson

### Keywords:

cosmogenic nuclides

Monte Carlo methods

snow shielding

low-energy neutron capture

## ABSTRACT

Conventional formulations of changes in cosmogenic nuclide production rates with snow cover are based on a mass-shielding approach, which neglects the role of neutron moderation by hydrogen. This approach can produce erroneous correction factors and add to the uncertainty of the calculated cosmogenic exposure ages. We use a Monte Carlo particle transport model to simulate fluxes of secondary cosmic-ray neutrons near the surface of the Earth and vary surface snow depth to show changes in neutron fluxes above rock or soil surface. To correspond with shielding factors for spallation and low-energy neutron capture, neutron fluxes are partitioned into high-energy, epithermal and thermal components. The results suggest that high-energy neutrons are attenuated by snow cover at a significantly higher rate (shorter attenuation length) than indicated by the commonly-used mass-shielding formulation. As thermal and epithermal neutrons derive from the moderation of high-energy neutrons, the presence of a strong moderator such as hydrogen in snow increases the thermal neutron flux both within the snow layer and above it. This means that low-energy production rates are affected by snow cover in a manner inconsistent with the mass-shielding approach and those formulations cannot be used to compute snow correction factors for nuclides produced by thermal neutrons. Additionally, as above-ground low-energy neutron fluxes vary with snow cover as a result of reduced diffusion from the ground, low-energy neutron fluxes are affected by snow even if the snow is at some distance from the site where measurements are made.

Published by Elsevier B.V.

## 1. Introduction

For over half a century the relationship between cosmogenic nuclide concentrations and landform ages has been explored (Davis and Schaeffer, 1955), and its application met with considerable success, with several nuclides ( $^3\text{He}$ ,  $^{10}\text{Be}$ ,  $^{14}\text{C}$ ,  $^{26}\text{Al}$ ,  $^{36}\text{Cl}$ ) used routinely to date landforms over Earth's surface (Muzikar et al., 2003). Recent efforts, such as the CRONUS project (Phillips, 2012), focus on reducing total methodological uncertainty to permit more precise and accurate assessment of ages and production rates. First- and second-order effects using physically-based parameterizations have been accounted for. These include the effects of erosion and inheritance (Lal, 1991), topographic shielding (Dunne et al., 1999), mass shielding (Cerling and Craig, 1994), spatio-temporal variability in cosmic-ray flux (Dunai, 2001; Desilets and Zreda, 2003; Lifton et al., 2005, 2008) and atmospheric pressure (Staiger et al., 2007). However, despite these successes, other uncertainties remain. One of these uncertainties, the effect of moisture at the land surface on cosmogenic production rates, is addressed here.

\* Corresponding author. Tel.: +1 520 621 4072; fax: +1 520 621 1422.  
E-mail address: czweck@hwr.arizona.edu (C. Zweck).

We use a Monte Carlo particle transport model to examine how snow affects secondary cosmic-ray neutron intensity near Earth's surface. Models such as these have been used to estimate rates of cosmogenic nuclide production (Masarik and Reedy, 1995) and other effects such as temporal changes in Earth's geomagnetic intensity (Masarik et al., 2001) and boulder size (Masarik and Wieler, 2003). Although snow cover represents only a small (10–15%) effect (Gosse and Phillips, 2001), it is considered necessary when dating boulders within moraine complexes, as the presence of moraines indicates recently glaciated environments. We place particular emphasis on low-energy neutron capture, which is a production pathway for  $^{36}\text{Cl}$ . Cosmogenic nuclide techniques give the 'apparent' age of a sample, the age computed under the assumption of continuous exposure at Earth's surface. If the period of exposure was punctuated by times when the sample was shielded, for example by soil, snow, ash or sand (Fig. 1), neutron fluxes and corresponding cosmogenic nuclide production rates near the surface will be affected. As a result, the apparent age will not be the same as the true exposure age, and a shielding correction factor must be computed to convert apparent age to exposure age. Covering materials can have a significant effect on computed exposure ages. For example Schildgen et al. (2005) estimate a spallation

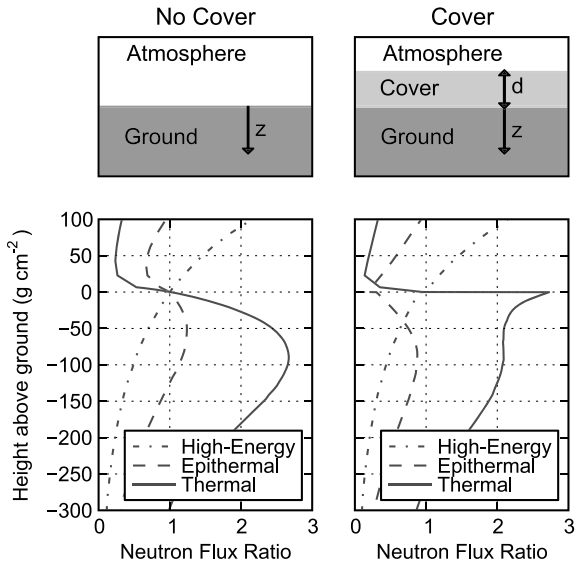


**Fig. 1.** The effect of ground cover on shielding of cosmic rays. Fluxes are normalized to unshielded surface values. Epithermal and thermal neutron fluxes also change above the snow surface (5 cm snow water equivalent) as a result of reduced net diffusion from the ground, which is not the case for high-energy neutron fluxes.

snow cover correction factor of 14% for a 15.5 ka sample from the Cairngorm Mountains in Scotland. Similarly, Gosse et al. (1995) present snow cover correction factors ranging from 0.6% to 15% for samples from the Wind River Range, Wyoming.

Prior research into the role of snow cover in moderating neutron fluxes is sparse, presumably because more rigorous formulations of snow scaling would be hampered by a lack of observational data regarding snow cover over the period of sample exposure. Generally, snow shielding is grouped into the more general category of mass shielding (Cerling and Craig, 1994; Schildgen et al., 2005), where the important characteristic of the shielding material is its ‘mass length’, reported as density times thickness ( $\text{g cm}^{-2}$ ). For cosmogenic nuclides generated by spallation, it is conventional to invoke a generic mass-shielding approach, in which the high-energy neutron flux beneath covering material  $\phi_{\text{cover}}$  is computed from (e.g. Gosse and Phillips, 2001, Eq. 3.75):

$$\frac{\phi_{\text{cover}}}{\phi} = e^{(-Z_{\text{cover}}/\Lambda_f)} \quad (1)$$

where  $\phi$  is the high-energy neutron flux ( $\text{neutrons cm}^{-2} \text{ yr}^{-1}$ ) in the absence of cover,  $Z_{\text{cover}}$  the mass length of the material covering the surface ( $\text{g cm}^{-2}$ ), and  $\Lambda_f$  the attenuation length for high-energy neutrons, thought to vary between  $140 \text{ g cm}^{-2}$  at Earth’s poles to  $170 \text{ g cm}^{-2}$  near the equator (Cerling and Craig, 1994), as Earth’s magnetic field blocks fewer low-energy, less penetrating cosmic rays near the poles.

For seasonal cover such as snow, the shielding factor  $S_{\text{snow}}$  is calculated as the sum of fractional components from a time discretization, such that in each time interval the cover can be assumed to be constant. For example monthly snow cover (e.g. Gosse and Phillips, 2001) is calculated as:

$$S_{\text{snow}} = \frac{\phi_{\text{snow}}}{\phi} = \frac{1}{12} \sum_i^{12} e^{-Z_{\text{snow},i} \rho_{\text{snow},i} / \Lambda_f} \quad (2)$$

where  $Z_{\text{snow},i}$  is the snow thickness during the  $i$ th month (cm) and  $\rho_{\text{snow},i}$  the density of snow during the  $i$ th month ( $\text{g cm}^{-3}$ ). Implicit in Eq. (2) is the notion that if the sample site is above the snowline, such as at the top of a large boulder, the sample can be considered snow free with no correction factor applied.

The above approach is reasonable for spallation because high-energy neutrons responsible for spallation reactions are attenuated by the mass length of materials above a dated surface. However, for low-energy neutrons, which are not only attenuated but also moderated, a different approach to correcting for snow cover is necessary.

## 2. Numerical simulations

To simulate changes in neutron flux resulting from changes in surface cover we use MCNPX (Monte Carlo N-Particle eXtended; Pelowitz, 2005) Version 2.5.0, a 3-D Monte Carlo particle transport code that can track 34 different particle types and more than 2000 heavy ions at nearly all energies. Interactions between neutrons and earth elements are computed using empirically derived, energy dependent cross sections of scattering and absorption; when these are not available, nuclear models are used.

In the simulations, Earth is approximated as a half space with 32 atmospheric layers and 43 subsurface layers. Atmospheric layers are composed of 22% oxygen and 78% nitrogen, have equal mass lengths of  $20 \text{ g cm}^{-2}$ , and extend from the surface to a height of 7.6 km. Atmospheric densities are computed from the pressure variation with height according to the International Standard Atmosphere (ISO 2533:1975) approximation.

Snow is represented as a surface layer of pure water with density  $1 \text{ g cm}^{-3}$ . Initial results with MCNPX showed statistical insignificance to variations in snow density, so we use water as a standard and report all results in terms of mass length (snow water equivalent in this case). Subsurface layers have uniform chemistries and densities, and are modeled as one of three possible types: siliceous dolomite, basalt, or granite (Supplementary Table S1).

In each MCNPX simulation,  $10^6$  neutrons are injected downwards into the uppermost atmospheric layer as the source function of incoming primary cosmic-ray flux, with an inverse power law energy spectrum (Grimani et al., 2011) over an energy  $E$  range between 6 GeV and 100 GeV as the source energy probability distribution. In the absence of a geomagnetic field, this energy spectrum emulates a low-latitude site (Roesler et al., 1998), with simulations using protons as primary cosmic-ray particles showing statistically insignificant differences to those using neutrons.

To reduce Monte Carlo uncertainties, MCNPX expresses neutron fluxes as ‘fluences’ ( $\text{neutrons cm}^{-2}$ ), defined as time integrated, volume averaged neutron fluxes normalized per unit source particle. Neutron fluences between different model simulations with the same geometry scale with each other in the same way as neutron fluxes. MCNPX partitions fluences into energy dependent bins, so that in any atmospheric or ground layer the neutron fluence within a pre-defined energy range can be estimated. In each layer, neutron fluences are partitioned into high-energy ( $100 \text{ MeV} < E < 200 \text{ MeV}$ ), epithermal ( $0.5 \text{ eV} < E < 10^{-3} \text{ MeV}$ ) and thermal ( $E < 0.5 \text{ eV}$ ) components. For a simulation using  $10^6$  neutrons as cosmic-ray source particles, we find that Monte Carlo uncertainties near the ground are typically smaller than 2%.

## 3. Results

In the absence of surface ground cover, high-energy neutron fluxes decrease exponentially with depth, whereas thermal and epithermal concentrations increase to reach broad maxima at depths between  $50 \text{ g cm}^{-2}$  and  $100 \text{ g cm}^{-2}$  (Liu et al., 1994; Phillips et al., 2001; Fig. 1 LHS). In the absence of any cover, the exponential attenuation with depth for high-energy neutrons is computed here as  $156 \text{ g cm}^{-2}$ , which for a cutoff rigidity of 6 GV compares reasonably with the  $170 \text{ g cm}^{-2}$  determined experimentally for  $^3\text{He}$  in basalt at ca. 13 GV by Kurz (1986). The difference

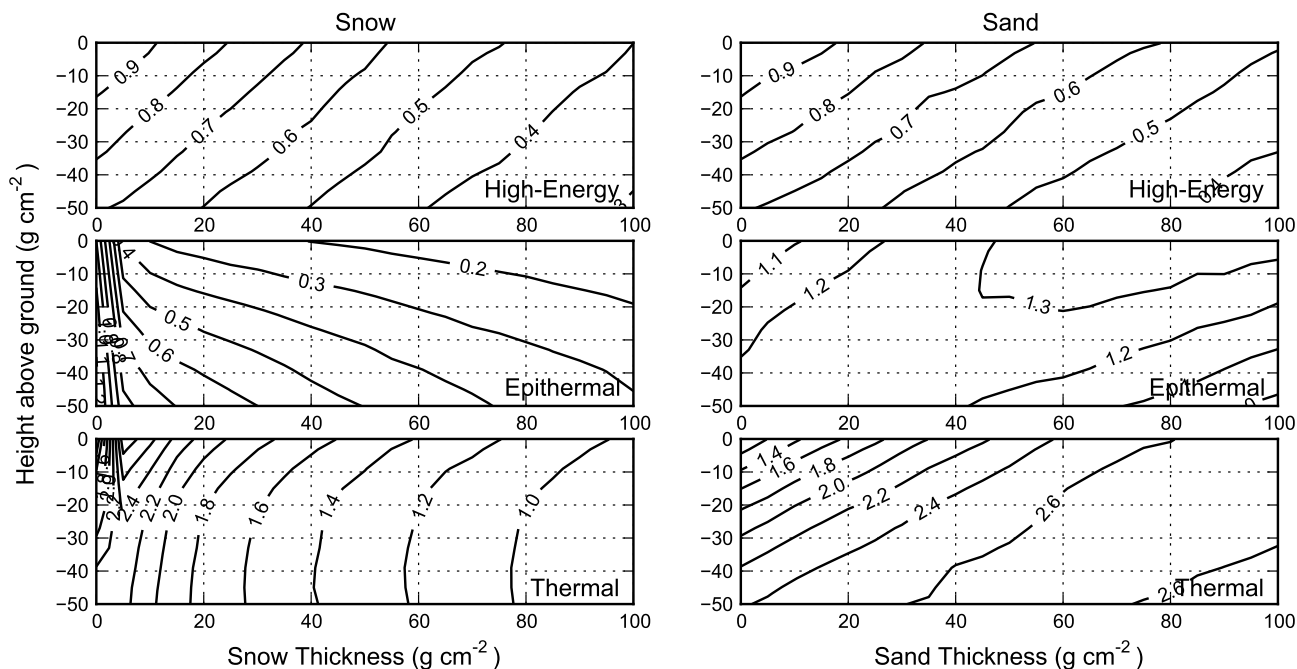


**Fig. 2.** Ratio of subsurface neutron fluxes to those without cover for snow cover (LHS) or sand cover (RHS). Fluxes are normalized to unshielded surface values. Snow is modeled as pure  $\text{H}_2\text{O}$  with density  $1.0 \text{ g cm}^{-3}$ ; sand is  $\text{SiO}_2$  with density  $1.0 \text{ g cm}^{-3}$ . The ground is modeled as basalt with density  $3 \text{ g cm}^{-3}$  and volumetric water content 0.5% (Supplementary Table S1).

in subsurface fluxes between high- and low-energy neutrons is a well known result (e.g., Fig. 3b in Liu et al., 1994; Fig. 3a in Gosse and Phillips, 2001) and is a combination of a) the generation of low-energy neutrons by the moderation of high-energy neutrons with b) the ground being a better moderator than the atmosphere. Rates of high-energy neutron moderation are at a maximum just below the ground surface, so that low-energy neutron fluxes reach a maximum here, with some diffusion back into the atmosphere (Liu et al., 1994).

For the case of snow cover (Fig. 1 RHS, 5 cm snow water equivalent) subsurface high-energy neutron fluxes decrease marginally, subsurface epithermal neutron fluxes decrease significantly with a deeper maximum, and thermal neutron fluxes display step-like behavior at the snowline, due to the increased moderation rate of high-energy neutrons by hydrogen in snow (Dep et al., 1994). Low-energy neutron fluxes are also reduced above the snowline, unlike the case for high-energy fluxes.

Hydrogen is a highly efficient moderator of neutrons, with average elemental moderating power approximately one order of magnitude larger than that of carbon (Fig. 5 and Table 1 in Zreda et al., 2012), the next most efficient moderator likely to be present in appreciable quantities in rocks and soils. As a result, neutron fluxes which are moderated by a surface cover containing hydrogen (snow, water, ice, vegetation, soil) differ to fluxes moderated by covering materials that do not contain comparable amounts of hydrogen (solid rocks, quartz sand). We note that most surfaces will have at least some amount of hydrogen in various pools, so the results that include hydrogen in surficial materials are more applicable to cosmogenic dating than are those without hydrogen. Fig. 2 shows subsurface neutron fluxes for basalt (Supplementary Table S1) when the ground is covered by snow (LHS) compared to quartzite sand (RHS), represented here as pure  $\text{SiO}_2$ . All neutron fluxes are normalized to surface, unshielded values. For high-energy neutron fluxes, the diagonal contours show the justification for shielding formulations of the type given by Eq. (1), in that for high-energy neutrons the flux attenuation resulting from surface cover is qualitatively the same as the attenuation with depth. However, for the same mass length of surface cover, snow moder-

ates high-energy fluxes more efficiently than either sand (cover) or basalt (depth). For a cover of  $100 \text{ g cm}^{-2}$ , snow reduces modeled high-energy neutron fluxes at the ground surface to about 40% of their cover-free values, compared with 52% for sand. When used in Eq. (1), these moderation rates imply attenuation lengths  $\Lambda_f$  of  $109 \text{ g cm}^{-2}$  for snow and  $153 \text{ g cm}^{-2}$  for sand, similar to the computed value of  $156 \text{ g cm}^{-2}$  for basalt (Fig. 1). This result suggests that mass-shielding corrections such as Eq. (1), which assume that ‘shielded’ samples can be treated analogously to ‘deeper’ samples underestimate the attenuation of high-energy neutron fluxes for snow. To verify this, we also conducted shielding simulations using basalt (not shown), and determined a shielding attenuation length of  $156 \text{ g cm}^{-2}$ , identical to the attenuation length computed for an unshielded sample (Fig. 1).

The correspondence in neutron attenuation between depth and cover for high-energy neutron fluxes does not extend to low-energy neutron fluxes (Fig. 2). Changes with depth of epithermal and thermal neutron fluxes are qualitatively different from those for high-energy fluxes, implying that Eq. (1) is inappropriate to calculate snow-shielding for nuclides produced by low-energy neutron capture (e.g. Benson et al., 2004). In our simulations, near-surface thermal neutron fluxes rapidly increase with snow cover to a mass length of about  $5 \text{ g cm}^{-2}$ . Compared to snow, much greater mass lengths of sand are required to increase thermal neutron fluxes to the same extent, with more epithermal neutrons present than for snow. This is likely a result of epithermal neutrons being more efficiently absorbed by snow than by quartz.

These results suggest that when dating using cosmogenic nuclides produced by low-energy neutron capture reactions, scaling factors for snow cover are dependent on the energy of the interacting neutron, and cannot be generalized to the form of Eq. (1). Using the formalism of Phillips et al. (2001), low-energy neutron capture production rates are separated into epithermal and thermal components, which are linearly dependent on epithermal and thermal neutron fluxes:

$$P_n = P_{eth} + P_{th} = \frac{f_{eth}}{\Lambda_{eth}} \phi_{eth} + \frac{f_{th}}{\Lambda_{th}} \phi_{th} \quad (3)$$

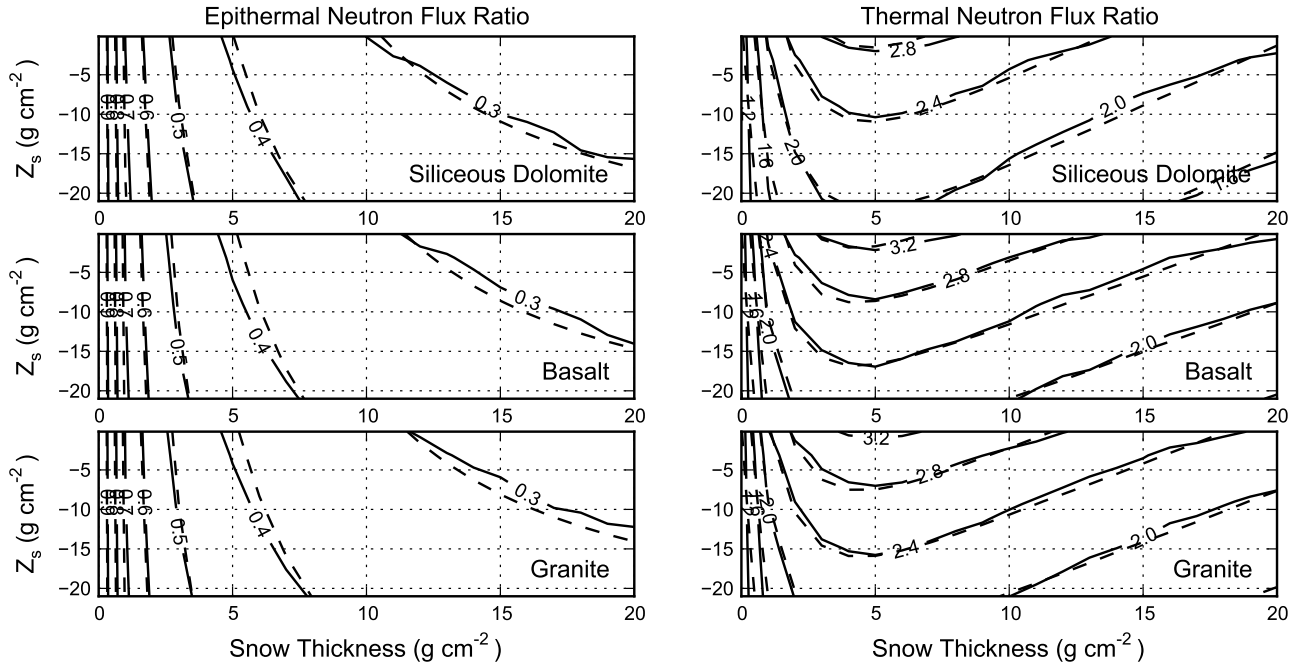


**Fig. 3.** Ratio of subsurface fluxes of epithermal (LHS) and thermal (RHS) neutrons to those at the same depth without snow cover, for sample types listed in each panel. Dashed lines show contours when Eqs. (6) and (7) are used to parameterize flux ratios.

**Table 1**

Parameters and 95% confidence intervals used in Eqs. (6) and (7), for siliceous dolomite, basalt, and granite (Supplementary Table S1).

Epithermal	$a_1$	$a_2$	$a_3$	$a_4$	
Siliceous dolomite	$1.51 \pm 0.13$	$-0.428 \pm 0.014$	$0.37 \pm 0.12$	$740 \pm 220$	
Basalt	$1.87 \pm 0.20$	$-0.388 \pm 0.015$	$0.46 \pm 0.16$	$1000 \pm 430$	
Granite	$1.81 \pm 0.18$	$-0.391 \pm 0.014$	$0.44 \pm 0.15$	$930 \pm 350$	
Thermal	$b_1$	$b_2$	$b_3$	$b_4$	$b_5$
Siliceous dolomite	$3.374 \pm 0.060$	$-0.0251 \pm 0.0013$	$-2.228 \pm 0.069$	$-0.611 \pm 0.040$	$1.0166 \pm 0.0006$
Basalt	$3.786 \pm 0.057$	$-0.0233 \pm 0.0011$	$-2.604 \pm 0.073$	$-0.745 \pm 0.046$	$1.0194 \pm 0.0006$
Granite	$3.701 \pm 0.056$	$-0.0238 \pm 0.0011$	$-2.525 \pm 0.069$	$-0.697 \pm 0.041$	$1.0185 \pm 0.0005$

where  $P_n$  is the total low-energy neutron capture production rate (atoms  $\text{g}^{-1} \text{yr}^{-1}$ ),  $P_{eth}$  and  $P_{th}$  the epithermal and thermal production rates (atoms  $\text{g}^{-1} \text{yr}^{-1}$ ),  $f$  is the fraction of either epithermal ( $f_{eth}$ ) or thermal ( $f_{th}$ ) neutrons which are absorbed by the target nuclide,  $\Lambda$  is the effective epithermal ( $\Lambda_{eth}$ ) or thermal ( $\Lambda_{th}$ ) attenuation length ( $\text{g cm}^{-2}$ ) and  $\phi$  the epithermal ( $\phi_{eth}$ ) or thermal ( $\phi_{th}$ ) neutron flux (neutrons  $\text{cm}^{-2} \text{yr}^{-1}$ ). As the variation of production rates with the amount of snow differs between thermal and epithermal neutron fluxes (Fig. 2), and also varies with subsurface depth, snow-corrected production rates should be of the form:

$$P_n = Q_{s,eth} P_{eth} + Q_{s,th} P_{th} \quad (4)$$

where  $Q_s$  is a sample depth-averaged snow shielding factor for thermal ( $Q_{s,th}$ ) and epithermal ( $Q_{s,eth}$ ) neutron production terms. For a sample extracted from the ground surface with thickness  $Z_s$  ( $\text{g cm}^{-2}$ ):

$$Q_s = \frac{1}{Z_s} \int_0^{Z_s} \frac{\phi_{cover}}{\phi} dz \quad (5)$$

Unfortunately,  $Q_s$  not only varies between thermal and epithermal neutron fluxes but also with ground chemistry (Fig. 3). We show results for the three different modeled sample chemistries (lithologies listed in Supplementary Table S1). In general, epithermal neutron flux ratios do not vary significantly for the different

sample types. This is expected because for most elements, absorption cross sections tend to decrease with increasing neutron energy, so that interaction probability is lower for epithermal neutrons than thermal neutrons (Glasstone and Edlund, 1952), with a corresponding decrease in sensitivity to chemical composition.

Through trial and error we found that the variation of depth-integrated neutron flux ratios with snow cover can be parameterized as follows (Fig. 3 dashed lines):

$$Q_{s,eth} = \frac{\phi_{s,eth}}{\phi_{eth}} = (a_1 Z_{cover} + 1)^{a_2} - \left( \frac{Z_s (Z_{cover})^{a_3}}{a_4} \right) \quad (6)$$

$$Q_{s,th} = \frac{\phi_{s,th}}{\phi_{th}} = (b_1 e^{b_2 Z_{cover}} + b_3 e^{b_4 Z_{cover}}) b_5^{-Z_s} \quad (7)$$

where  $Z_{cover}$  is the snow mass length ( $\text{g cm}^{-2}$ ) and  $a_1, \dots, a_4, b_1, \dots, b_5$  are fitting coefficients which depend on lithology (Table 1). Ideally the parameterizations should be a function of the exact chemistry of the sample being dated. However, as histories of snow cover at any given sample location likely have a larger uncertainty than chemistry dependent production rate variations, it suffices to consider the parameterization by rock type, as we did above, especially given the similarity in results. We make no claim regarding the uniqueness or goodness-of-fit of these parameterizations to the modeled fluxes, but note that they appear to reproduce the simulations reasonably well, with most uncertainties below 10% (Table 1).

#### 4. Discussion

As mentioned in the introduction, the utility of revising snow attenuation factors for spallation and low-energy neutron capture is hampered by a lack of observational data of past snow cover. However, differences between the formulations can give some insight into our understanding of real versus apparent cosmogenic sample ages. For example, the 14% snow correction factor for an 11.5 ka sample from the Cairngorm Mountains (Schildgen et al., 2005) is based on Eq. (1) with  $\Delta_f = 165 \text{ g cm}^{-2}$ , from which we could infer an 'effective' or 'apparent' snow cover of  $25 \text{ g cm}^{-2}$ . Combining this snow cover with  $\Delta_f = 109 \text{ g cm}^{-2}$  gives a snow scaling factor of 20%, inferring that nuclides generated predominantly via spallation underestimate the effects of snow cover by up to 40%.

For  $^{36}\text{Cl}$ , the role of snow cover is more complex and more significant. For the Cairngorm Mountains example, boulders within moraines are most likely to be granite (Phillips et al., 2006). Although the flux of low-energy neutrons within granite is very similar to other lithologies (Fig. 3, Table 1), the rate of cosmogenic production from low-energy neutron capture is very sensitive to sample chemistry (Phillips et al., 2001), and for the lithologies presented in Supplementary Table S1 the percentage of total cosmogenic production from low-energy neutron capture would be 40% for siliceous dolomite, 44% for granite and 57% for basalt (Zweck et al., 2012). For granite, capture of epithermal neutrons is 14% of total production, and capture of thermal neutrons is 30% of total production. For the sake of example, if we assume that a boulder from the Cairngorm Mountains had identical chemical composition as that of granite in Supplementary Table S1, the previous paragraph would indicate a decrease in spallation production rates of 20% for  $25 \text{ g cm}^{-2}$  of snow. For low-energy neutrons, a sample thickness  $Z_s$  of  $5 \text{ g cm}^{-2}$  would produce an 80% decrease in epithermal neutron fluxes and an 80% increase in thermal neutron fluxes (Eqs. (6) and (7)). This almost doubling of neutron fluxes for a process responsible for 30% of total production means that the  $25 \text{ g cm}^{-2}$  snow shielded  $^{36}\text{Cl}$  inventory would be slightly more (1.6%) than it would in the absence of any snow cover. However it should be stressed that this is only for a hypothetical  $^{36}\text{Cl}$  sample with assumed snow cover and chemical composition, and that other combinations and snow cover and chemical composition will have different snow scalings.

##### 4.1. Implications for surfaces above snow level

As thermal and epithermal neutrons diffuse back into the atmosphere (Phillips et al., 2001; Glasstone, 1955) their fluxes vary both above and below the snow pack (Fig. 1). An important implication is that, contrary to Eq. (2), cosmogenic nuclides produced by low-energy neutrons will be affected by snow regardless of whether rock surfaces are above or below the snowline. Subsurface thermal and epithermal neutron concentrations vary significantly below snow layers, mainly due to variations in soil/rock chemistry and its water content. The snow pack adds to this variation.

Fig. 4 shows neutron ratios from snow-free conditions 1–2 m above the ground as a function of snow thickness. High-energy neutron fluxes above the snow surface are unaffected by snow cover because all neutrons in this component originate from the atmosphere, and can be thought of as moving as a beam (Gosse and Phillips, 2001). But epithermal fluxes are significantly reduced and thermal fluxes significantly increased for even small thicknesses of snow, as a result of moderation by hydrogen. As epithermal neutrons are slowed by collisions with hydrogen atoms, they are removed from a given energy range, and their intensity in this energy bin decreases. These neutrons are then shifted to lower-energy bins, and the intensity of thermal neutrons increases.

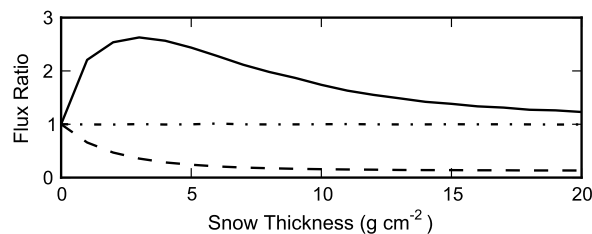


Fig. 4. Modeled fluxes of high-energy (dot-dashed), epithermal (dashed) and thermal (solid) neutron fluxes averaged between 1 and 2 m above the ground as a function of snow thickness ( $\text{g cm}^{-2}$ ). Fluxes are shown as ratios from uncovered values for each energy range.

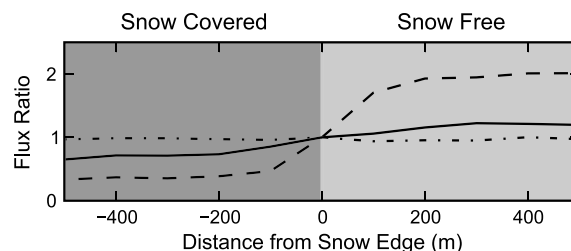


Fig. 5. Modeled fluxes of high-energy (dot-dashed), epithermal (dashed) and thermal (solid) neutron fluxes averaged between 1 and 2 m above the ground as a function of horizontal distance from a block of snow  $1 \text{ km} \times 1 \text{ km} \times 20 \text{ g cm}^{-2}$  thick. Fluxes are shown as ratios from values at the snow edge for each energy range.

As the mean free path in the atmosphere of epithermal and thermal neutrons is hectometers and dekameters, respectively (Hess, 1959), and the velocity of neutrons is at least several kilometers per second (Zreda et al., 2012), atmospheric neutron concentrations above the ground or snow surface tend to be well mixed over these spatial scales. This suggests that sites not just below snow (or ice or water or any other source of hydrogen), but also those near any body of hydrogen will have their flux of low-energy neutrons affected. As an example, for the hypothetical granite boulder discussed in the previous section, the total production rate will be 10% lower than in snow free conditions, even if the boulder is above the snow line and the top of the boulder is snow free, as a result of the decrease in epithermal neutron flux (Fig. 4). An important simplification that persists in cosmogenic literature is that even in the presence of snow, tops of tall boulders are likely to be snow-free because snow is quickly removed from boulder tops by the wind (e.g. Schimmelpfennig et al., 2011). But even if this tall boulder that always remains free of snow is surrounded by snow on the ground, the low-energy neutron intensity will be a strong function of the amount of snow (or snow-water equivalent), and the production rates of cosmogenic isotopes produced by neutron activation will be affected in a way shown in Fig. 4.

##### 4.2. Other sources of hydrogen

The same analysis applies to boulders embedded in fine matrix, such as glacial erratics in moraine matrix. Such a matrix is likely to have amounts of water that vary in time, for example reflecting seasonal changes or longer-term trends. Even if boulder tops are above the surface of the matrix, the low-energy neutron flux on top of the boulder will depend on the average soil moisture within hundreds of meters around the boulder (Hess, 1959; Zreda et al., 2008), and the production rates will vary in time accordingly.

A vertical wall of a valley that has snow at the bottom will be affected by this snow. Replace snow with soil (with soil water), a river or a lake, or even dense vegetation, and the neutron intensity on the wall will be affected. The effect will reduce exponentially with distance from the source of hydrogen.

Similarly, areas at or near shorelines will have the low-energy neutron flux affected by the water. Halfspace simulations focusing on a boulder top at variable distance from a  $1 \text{ km} \times 1 \text{ km} \times 20 \text{ g cm}^{-2}$  body of water show that thermal and epithermal neutron fluxes still vary hundreds of meters away from hydrogen-free conditions (Fig. 5). Situations such as river terraces, marine shorelines or paleo-lake shorelines will require appropriate corrections to production rates by low-energy neutron activation.

#### 4.3. Implications for cosmogenic dating

It is important to know how far the influence of snow (or other near-surface source of hydrogen) extends in the air above the land surface. As noted before the mean free path for epithermal neutrons is a few hundred meters and that of thermal neutrons a few tens of meters, both at sea level (Hess, 1959). This means that neutrons in air are well mixed at these length scales, and therefore, that any perturbation in the moderating or absorption properties of the material at the Earth's surface will be propagated approximately these distances, with an exponentially decreasing sensitivity, as described in the context of measuring soil moisture with cosmic-ray neutrons (Zreda et al., 2008, 2012). Thus, any source of hydrogen (snow, water, vegetation, etc.) that is present within tens to hundreds of meters from the dated surface will affect thermal and epithermal neutron intensities (Figs. 4 and 5) and thus the production rates and calculated apparent ages of landforms.

The above conditions will affect exposure ages obtained from cosmogenic nuclides produced by low-energy neutrons. But a part of the effect can be removed during calibration. Most calibration samples come from environments that have near-surface hydrogen in the form of soil moisture, vegetation, snow, lattice (mineral) water or surface water bodies. Therefore, most calibrated production rates will have the effect of near-surface hydrogen included implicitly (or built in). The variable levels of near-surface hydrogen content for different calibration samples will manifest themselves in a spread of calculated single-sample production rates, and the larger spread will be expected of data sets that include a broader range of environments. Thus, in order to reduce the uncertainty in the calculated production rates, we should not seek more samples or seek samples from drier environments, which are preferred for cosmogenic dating. Instead, we should implement a more proper evaluation of the environmental hydrogen for all calibration and application samples.

That could be done in a way suggested for measuring present-day soil moisture with cosmic-ray neutrons, where pools of hydrogen other than that in soil pore water had to be identified and quantified (Zreda et al., 2012). But this is difficult to do for geological past. A good and practical alternative is to use calibration samples from a broader range of environments. This will produce a data set with a larger variance of the calibrated production rates with the correspondingly larger uncertainty on the computed cosmogenic exposure ages. But the bias due to any systematic differences between calibration samples and application samples will be minimized.

#### 4.4. A possibility of inferring past moisture levels

The high sensitivity of low-energy neutrons to the presence of hydrogen has been used to measure soil moisture at the horizontal scale of hundreds of meters (Zreda et al., 2008). This is now being extended to measuring other pools of hydrogen at the Earth's surface, such as atmospheric moisture, snow and vegetation (Zreda et al., 2012). Desilets et al. (2010) have suggested the possibility of extending these measurements to assessing surface moisture in the recent geological past by using proxies for neutrons. Such proxies are cosmogenic nuclides that have been used to date landforms

and other features at the Earth's surface (e.g., Gosse and Phillips, 2001). Here is how it might work:

Under ideal conditions, with no erosion, no shielding, no prior exposure and unbiased calibrations, all cosmogenic isotopes should produce the same apparent age of landforms. When conditions are changed in such a way that different nuclides are affected differently, these nuclides will give different apparent ages. If the difference is larger than could be explained by analytical uncertainties, it can be attributed to a geological process that modified the cosmogenic production and accumulation. A well-known example is the potential use of two isotopes with different half-lives, typically  $^{10}\text{Be}$  and  $^{26}\text{Al}$ , to determine both the exposure time and the erosion rate (Lal, 1991). A less known potential application is the use of a long-lived nuclide (such as  $^{36}\text{Cl}$ ) with a very short lived one ( $^{14}\text{C}$ ) to quantify multiple exposure episodes and the intervening burial episodes (Zreda and Lifton, 2005). In the same spirit we propose to use cosmogenic isotopes produced by spallation (high energy) and by neutron activation (low energy) to determine the exposure time and the effective (time-integrated) surface moisture.

The production rate of the spallogenic nuclide will be affected only by the presence of surface moisture that forms a cover on the dated surface (for example snow); if the moisture does not cover the sample site, the production rate is unaffected. In contrast, as discussed above and illustrated in Figs. 2–5, nuclides produced by neutron activation will be strongly affected by moisture that is either directly on top of the dated surface or nearby. Because the thermal neutron intensity increases significantly when moisture is present (Figs. 4–5), and most of the production is by thermal rather than epithermal neutrons, the neutron activation production rate increases and as a result the accumulated nuclide inventory will be larger than in the case without surface moisture. Thus, the apparent age will be older than that computed from the spallogenic nuclide. The difference between the two, if attributable to moisture, can be used to compute the average moisture level over the entire exposure time of the landform.

This is a simple proposal, and it has caveats. One is that production rates of neutron activation produced nuclides can increase due to another process: erosion of the landform surface. This is due to the distribution of thermal neutrons below the ground surface, with a maximum at a depth less than  $100 \text{ g cm}^{-2}$ . Erosion will progressively (or episodically) remove the surface layers and expose those subsurface layers that experienced higher production rates before. Under slow erosion rates the nuclide inventory in eroding landforms will be larger than that in non-eroding landforms, making this effect similar to that of surface moisture. The effect on the spallogenic nuclide is always such that the inventory is smaller than in non-eroding landforms, again similar to the effect of moisture that covers the surface. Thus, the two complications, due to moisture and due to erosion, will have a similar effect on the ratio of activation to spallation inventories, making it impossible uniquely to attribute the ratio to either one. However, if one of the two complications could be assessed independently, or eliminated, the system would become tractable with two nuclides.

Erosion is probably easier than moisture to be assessed independently. For example, it can be determined, in principle at least, using two spallogenic nuclides (Lal, 1991). Based on the erosion rates, the inventory of the neutron-activation nuclide could be corrected for erosion, and the apparent age computed. Any remaining difference between the spallogenic age and the activation age is now attributable to surface moisture.

Another possibility is to identify surfaces that show no evidence of erosion after deposition, for example glacial striae (Fogwill et al., 2004) or fine texture on lava flows (Desilets and Zreda, 2006). On these surfaces any difference between spallogenic and neutron activation inventories can be attributable to surface moisture. Of course, the presence of striae or fine texture on lava flows does

not guarantee that there was no erosion. Striae could be preserved under a layer of sediment and only recently exposed at the surface. Similarly, fine texture on lava tops could be exposed by spalling a surface layer of lava immediately above it. In addition, these surfaces may have had some covering material (sand, soil) that was removed at some time, which would complicate the determination of paleo moisture. Sampling from a steep valley wall a few meters above the valley bottom could minimize these complications, while still providing the opportunity to compare spallogenic and thermal neutron produced nuclides and derive past moisture levels.

## 5. Conclusions

As water contains hydrogen, a highly efficient moderator of secondary cosmic-ray neutrons, cosmogenic nuclide production rates for samples shielded by snow, ice or water differ to those for other shielding types, such as sand, soil or ash. This is especially true for nuclides which have an appreciable production component by low-energy neutrons, such as  $^{36}\text{Cl}$ . Our modeling results indicate that for spallation a 30% reduction, compared with rock, in attenuation length is sufficient to account for snow. However, for low-energy neutrons more complicated parameterizations are required, particularly for samples from low snow-fall areas where neutron fluxes can reach up to 3 times their unshielded values. A limiting factor in the accuracy of correction factors for snow attenuation is knowledge of past histories of snow density and depth over the exposure duration, so the parameterizations should be used predominantly to explore the sensitivity of computed ages to snow depth variations. For better understood sample locations, this result offers the intriguing possibility that multiple nuclide analysis involving  $^{36}\text{Cl}$  with a spallation-only nuclide could provide some insight into the site history of regional soil wetness. Samples from regions with extremely low precipitation, such as the Dry Valleys, Antarctica or Atacama Desert, Chile would be ideal to examine this hypothesis, although erosion would still need to be considered (e.g. Middleton et al., 2012).

An important result from the simulations is that for  $^{36}\text{Cl}$ , nuclide concentrations are affected not only if the surfaces are under a cover of snow (ice, water, vegetation), but also if they are in the vicinity of any source of hydrogen. This is because above surface thermal and epithermal neutron concentrations depend on below surface concentrations of these neutrons, and these concentrations vary with hydrogen concentrations at and near the surface.

## Acknowledgements

Research supported by the US National Science Foundation (grants 0325929, 0345440, 0636110 and 0838491). Sandia National Laboratories is a multi-program laboratory managed and operated by Sandia Corporation, a wholly owned subsidiary of Lockheed Martin Corporation, for the U.S. Department of Energy's National Nuclear Security Administration under contract DE-AC04-94AL85000. We would like to thank Patrick Applegate and an anonymous reviewer for providing thoughtful and constructive reviews.

## Appendix A. Supplementary material

Supplementary material related to this article can be found online at <http://dx.doi.org/10.1016/j.epsl.2013.07.023>.

## References

- Benson, L., Madole, R., Phillips, W., Landis, G., Thomas, T., Kubik, P., 2004. The probable importance of snow and sediment shielding on cosmogenic ages of north-central Colorado Pinedale and pre-Pinedale moraines. *Quat. Sci. Rev.* 23 (1–2), 193–206.
- Cerling, T.E., Craig, H., 1994. Geomorphology and in-situ cosmogenic isotopes. *Annu. Rev. Earth Planet. Sci.* 22 (1), 273–317.
- Davis, J., Schaeffer, O., 1955. Chlorine-36 in nature. *Ann. N.Y. Acad. Sci.* 62, 105–122.
- Dep, L., Elmore, D., Fabryka-Martin, J., Masarik, J., Reedy, R.C., 1994. Production rate systematics of in-situ-produced cosmogenic nuclides in terrestrial rocks: Monte Carlo approach of investigating  $^{35}\text{Cl}(n, \gamma)^{36}\text{Cl}$ . *Nucl. Instrum. Methods Phys. Res., Sect. B, Beam Interact. Mater. Atoms* 92 (1–4), 321–325.
- Desilets, D., Zreda, M., 2003. Spatial and temporal distribution of secondary cosmic-ray neutron intensities and applications to in situ cosmogenic dating. *Earth Planet. Sci. Lett.* 206 (1–2), 21–42.
- Desilets, D., Zreda, M., 2006. Elevation dependence of cosmogenic  $^{36}\text{Cl}$  production in Hawaiian lava flows. *Earth Planet. Sci. Lett.* 246, 277–287.
- Desilets, D., Zreda, M., Ferre, T., 2010. Nature's neutron probe: Land-surface hydrology at an elusive scale with cosmic rays. *Water Resour. Res.* 46, W011505, <http://dx.doi.org/10.1029/2009WR008726>.
- Dunai, T.J., 2001. Influence of secular variation of the geomagnetic field on production rates of in situ produced cosmogenic nuclides. *Earth Planet. Sci. Lett.* 193 (1–2), 197–212.
- Dunne, J., Elmore, D., Muzikar, P., 1999. Scaling factors for the rates of production of cosmogenic nuclides for geometric shielding and attenuation at depth on sloped surfaces. *Geomorphology* 27 (1–2), 3–11.
- Fogwill, C.J., Bentley, M.J., Sugden, D.E., Kerr, A.R., Kubik, P.W., 2004. Cosmogenic nuclides  $^{10}\text{Be}$  and  $^{26}\text{Al}$  imply limited Antarctic Ice Sheet thickening and low erosion in the Shackleton Range for >1 m.y. *Geology* 32 (3), 265–268.
- Glasstone, S., 1955. Principles of Nuclear Reactor Engineering. With the assistance of ORNL staff members, E.E. Anderson and others. Van Nostrand, New York, 861 pp.
- Glasstone, S., Edlund, M.C., 1952. The Elements of Nuclear Reactor Theory. Van Nostrand, Princeton, NJ, 416 pp.
- Gosse, J., Phillips, F., 2001. Terrestrial in situ cosmogenic nuclides: theory and application. *Quat. Sci. Rev.* 20, 1475–1560.
- Gosse, J.C., Evenson, E.B., Klein, J., Lawn, B., Middleton, R., 1995. Precise cosmogenic  $^{10}\text{Be}$  measurements in western North America: Support for a global Younger Dryas cooling event. *Geology* 23 (10), 877–880.
- Grimani, C., Araújo, H.M., Fabi, M., Lobo, A., Mateos, I., Shaul, D.N.A., Sumner, T.J., Wass, P., 2011. Galactic cosmic-ray energy spectra and expected solar events at the time of future space missions. *Class. Quantum Gravity* 28 (9), 094005.
- Hess, W.N., Patterson, H.W., Wallace, R., Chupp, E.L., 1959. Cosmic-ray neutron energy spectrum. *Phys. Rev.* 116 (2), 445–457.
- Kurz, M.D., 1986. In situ production of terrestrial cosmogenic helium and some applications to geochronology. *Geochim. Cosmochim. Acta* 50, 2855–2862.
- Lal, D., 1991. Cosmic ray labeling of erosion surfaces: in situ nuclide production rates and erosion models. *Earth Planet. Sci. Lett.* 104 (2), 424–439.
- Lifton, N.A., Bieber, J.W., Clem, J.M., Duldig, M.L., Evenson, P., Humble, J.E., Pyle, R., 2005. Addressing solar modulation and long-term uncertainties in scaling secondary cosmic rays for in situ cosmogenic nuclide applications. *Earth Planet. Sci. Lett.* 239, 140–161.
- Lifton, N., Smart, D.F., Shea, M.A., 2008. Scaling time-integrated in situ cosmogenic nuclide production rates using a continuous geomagnetic model. *Earth Planet. Sci. Lett.* 268 (1–2), 190–201.
- Liu, B., Phillips, F.M., Fabryka-Martin, J.T., Fowler, M.M., Stone, W.D., 1994. Cosmogenic  $^{36}\text{Cl}$  accumulation in unstable landforms 1. Effects of the thermal neutron distribution. *Water Resour. Res.* 30 (11), 3115–3125.
- Masarik, J., Reedy, R.C., 1995. Terrestrial cosmogenic-nuclide production systematics calculated from numerical simulations. *Earth Planet. Sci. Lett.* 136 (3–4), 381–395.
- Masarik, J., Wieler, R., 2003. Production rates of cosmogenic nuclides in boulders. *Earth Planet. Sci. Lett.* 216 (1–2), 201–208.
- Masarik, J., Frank, M., Schafer, J.M., Wieler, R., 2001. Correction of in situ cosmogenic nuclide production rates for geomagnetic field intensity variations during the past 800,000 years. *Geochim. Cosmochim. Acta* 65 (17), 2995–3003.
- Middleton, J.L., Ackert Jr., R.P., Mukhopadhyay, S., 2012. Pothole and channel system formation in the McMurdo Dry Valleys of Antarctica: New insights from cosmogenic nuclides. *Earth Planet. Sci. Lett.* 355–356, 341–350.
- Muzikar, P., Elmore, D., Granger, D.E., 2003. Accelerator mass spectrometry in geologic research. *Geol. Soc. Am. Bull.* 115 (6), 643–654.
- Pelowitz, D.B. (Ed.), 2005. MCNPX User's Manual, Version 2.5.0. Los Alamos National Laboratory report LA-CP-05-0369.
- Phillips, F., 2012. Cronus–Earth project: Results. *Quat. Int.* 279–280, 379, <http://dx.doi.org/10.1016/j.quaint.2012.08.1175>.
- Phillips, F.M., Stone, W.D., Fabryka-Martin, J.T., 2001. An improved approach to calculating low-energy cosmic-ray neutron fluxes near the land/atmosphere interface. *Chem. Geol.* 175 (3–4), 689–701.
- Phillips, W.M., Hall, A.M., Mottram, R., Fifield, L.K., Sugden, D.E., 2006. Cosmogenic  $^{10}\text{Be}$  and  $^{26}\text{Al}$  exposure ages of tors and erratics, Cairngorm Mountains, Scotland: Timescales for the development of a classic landscape of selective linear glacial erosion. *Geomorphology* 73 (3–4), 222–245.
- Roesler, S., Heinrich, W., Schraube, H., 1998. Calculation of radiation fields in the atmosphere and comparison to experimental data. *Radiat. Res.* 149 (1), 87–97.

- Schildgen, T.F., Phillips, W.M., Purves, R.S., 2005. Simulation of snow shielding corrections for cosmogenic nuclide surface exposure studies. *Geomorphology* 64 (12), 67–85.
- Schimmelpfennig, I., Benedetti, L., Garreta, V., Pik, R., Blard, P.-H., Burnard, P., Bourlès, D., Finkel, R., Ammon, K., Dunai, T., 2011. Calibration of cosmogenic  $^{36}\text{Cl}$  production rates from Ca and K spallation in lava flows from Mt. Etna (38°N, Italy) and Payun Matru (36°S, Argentina). *Geochim. Cosmochim. Acta* 75 (10), 2611–2632.
- Staiger, J., Gosse, J., Toracinta, R., Oglesby, B., Fastook, J., Johnson, J.V., 2007. Atmospheric scaling of cosmogenic nuclide production: Climate effect. *J. Geophys. Res., Solid Earth* 112 (B2), B02205.
- Zreda, M., Lifton, N., 2005. In-situ  $^{14}\text{C}$  and  $^{36}\text{Cl}$ : A tool for analyzing complex exposure and burial histories of glacial landscapes. In: Geological Society of America Annual Meeting, Salt Lake City, October 2005.
- Zreda, M., Desilets, D., Ferré, T.P.A., Scott, R.L., 2008. Measuring soil moisture content non-invasively at intermediate spatial scale using cosmic-ray neutrons. *Geophys. Res. Lett.* 35, L21402, <http://dx.doi.org/10.1029/2008GL035655>.
- Zreda, M., Shuttleworth, W.J., Zeng, X., Zweck, C., Desilets, D., Franz, T., Rosolem, R., 2012. COSMOS: The COsmic-ray Soil Moisture Observing System. *Hydrol. Earth Syst. Sci.* 16, 4079–4099, <http://dx.doi.org/10.5194/hessd-16-4079-2012>.
- Zweck, C., Zreda, M., Anderson, K.M., Bradley, E., 2012. The theoretical basis of ace, an age calculation engine for cosmogenic nuclides. *Chem. Geol.* 291, 199–205.